ELSEVIER

Biophysical Chemistry 63 (1997) 153–166

Biophysical Chemistry

Pulse radiolysis studies of intramolecular electron transfer in model peptides and proteins. 7. $Trp^{\cdot} \rightarrow TyrO^{\cdot}$ radical transformation in hen egg-white lysozyme Effects of pH, temperature, Trp62 oxidation and inhibitor binding

Krzysztof Bobrowski [a,b], Jerzy Holcman [c], Jaroslaw Poznanski [a], Kazimierz Lech Wierzchowski [a,*]

[a] *Institute of Biochemistry and Biophysics, Polish Academy of Sciences, 02-106 Warszawa, Poland*
[b] *Institute of Nuclear Chemistry and Technology, 03-195 Warszawa, Poland*
[c] *Department of Environmental Sciences, Risø National Laboratory, DK-4000 Roskilde, Denmark*

Received 24 June 1996; revised 2 September 1996; accepted 10 September 1996

Abstract

Intramolecular long-range electron transfer (LRET) in hen egg-white lysozyme (HEWL) accompanying $Trp^{\cdot} \rightarrow TyrO^{\cdot}$ radical transformation was investigated in aqueous solution by pulse radiolysis as a function of pH (5.2–7.4) and temperature (283–328 K). The reaction was induced by highly selective oxidation of Trp with $N_3^{\cdot}$ radicals under low concentration of the reactants but at a high HEWL/$N_3^{\cdot}$ molar ratio, so that more than 99% of the oxidized protein molecules contained only a single tryptophyl radical. Synchronous decay of $Trp^{\cdot}$ and build-up of $TyrO^{\cdot}$ conformed satisfactorily to first-order kinetics, indicating that LRET involved either one or more $Trp^{\cdot}$/Tyr redox pairs characterized by similar rate constants. The rate constant of LRET, k_5, increased monotonously with decreasing pH showing the following characteristics: (i) in the pH range 7.4–5.2 the plot of k_5 against pH was sigmoidal in shape, reflecting protonation of Glu35 ($pK_a \approx 6$) and pointing to involvement of conformational control of the kinetics of LRET, (ii) below pH 5.2 a sharp increase in k_5 was observed due to the protonation of $Trp^{\cdot}$ to form $TrpH^{\cdot+}$, which is known to oxidize tyrosine faster than does $Trp^{\cdot}$. Arrhenius plots of the temperature-dependence of k_5 showed that the activation energy of LRET varies both with temperature and the protonation state of the enzyme. The activation energies are in the range 7.6–56.0 kJ mol^{-1} and are similar to those for activation of amide hydrogen exchange in native HEWL below its denaturation temperature. Selective oxidation by ozone of the Trp62 indole side-chain in HEWL to *N'*-formylkynurenine (NFKyn62-HEWL) caused a large drop in the initial yield of $Trp^{\cdot}$ radicals, $G(Trp^{\cdot})_i$. This was accompanied by a relatively small decrease in k_5 but selective oxidation by ozone had a pronounced effect on its temperature-dependence. Taken together these observations indicate that of the six tryptophans present in HEWL Trp62 contributes about 50% to the yield of the observed LRET. In the enzyme–inhibitor complex, $HEWL(GlcNAc)_3$, where Trp62 and Trp63 are completely shielded from the solvent by the bound triacetylchitotriose, $G(Trp^{\cdot})_i$ was lower than in NFKyn62-HEWL, and both the kinetic and energetic characteristics of LRET, observed at pH 5.2, were again somewhat different than in HEWL alone. Considering known solvent accessibilities of tryptophans in the

* Corresponding author.

PII S0301-4622(96)02226-0

complex, the observed LRET process in HEWL$(GlcNAc)_3$ was assigned to Trp123. Theoretical evaluation of the electronic coupling for the dominant LRET pathways between all the potential $Trp^{\cdot}$/Tyr redox couples in HEWL, with help of the PATHWAYS model, enabled Trp62/Tyr53, Trp63/Tyr53 and Trp123/Tyr23 to be identified as the pairs involved in the experimentally observed electron transfer.

Keywords: Hen egg-white lysozyme; Intramolecular electron transfer; Pulse radiolysis; Radical transformation; Tryptophan radical; Tyrosine radical

1. Introduction

Efficient intramolecular radical transformation $Trp^{\cdot} \rightarrow TyrO^{\cdot}$, involving long-range electron transfer (LRET) between the phenol side-chain of Tyr and the $Trp^{\cdot}$ indolyl radical, has been observed in a number of proteins [1–4], including hen egg-white lysozyme (HEWL) [2–4], and in model systems made of a single Trp/Tyr pair separated by a peptide bridge [5–14]. Such a long-range unpaired electron transfer may extend the target size for radiation-induced damage of sub-cellular protein structures (cf. [11] and references cited therein). Evidence is also accumulating that tyrosine and tryptophan radicals are involved in electron transfer associated with physiological redox reactions: $Trp^{\cdot} \rightarrow TyrO^{\cdot}$ transformation can be an important step in the catalytic mechanisms of H_2O_2/cytochrome c–peroxidase complex [15–17], $TyrO^{\cdot}$ has been implicated as a reaction intermediate in the photosystem II [18], ribonucleotide reductase [19] and prostaglandin synthase [20]. Further studies on LRET in HEWL, as a model protein system for $Trp^{\cdot} \rightarrow TyrO^{\cdot}$ transformation, are, therefore, worth continuing. So far, however, it has proved impossible to identify which of the potential $Trp^{\cdot}$/Tyr redox pairs, formed by six tryptophan and three tyrosine residues present in HEWL, and which of the associated molecular pathways were actually involved in the observed LRET. Our preliminary pulse radiolysis study on the temperature-dependence of LRET in HEWL [3] showed close similarity between the Arrhenius plots for the kinetics of this process and the specific enzymatic reaction of HEWL, suggesting that similar thermally induced conformational fluctuations are involved in the activation of the two processes in lysozyme. If this is true, then the fluctuations of significance for intramolecular electron transfer must affect conformational motions of tryptophan and/or tyrosine residues engaged in the binding of substrates or located in the proximity of substrate binding sites in the active centre of the enzyme. In HEWL, three tryptophan residues: Trp62, Trp63, and Trp108 are located in the active site of the enzyme and are involved in the binding of oligosaccharide-type substrates [21]. In view of the highly selective and very efficient oxidation of Trp to $Trp^{\cdot}$ in HEWL by $N_3^{\cdot}$ radicals [2–4], involvement of Trp62, Trp123 and Trp63 residues, which are most solvent-accessible, in the oxidation and LRET reactions has been suggested [4]. This hypothesis finds support in the fact that the indole ring of Trp62 can be selectively oxidized to *N'*-formylkynurenine (NFKyn) by ozone [22,23].

To identify which of the potential $Trp^{\cdot}$/Tyr redox pairs are actually involved in the $N_3^{\cdot}$-induced $Trp^{\cdot} \rightarrow TyrO^{\cdot}$ transformation in HEWL, we performed further pulse radiolysis studies of this reaction in: (i) the native enzyme, (ii) the complex of HEWL with an oligosaccharide inhibitor, triacetylchitotriose, and (iii) HEWL selectively oxidized by ozone to the NFKyn62 derivative. Both temperature- and pH-dependent perturbations of the HEWL structure were investigated. The results obtained are interpreted in terms of the most probable LRET pathways between various $Trp^{\cdot}$/Tyr redox pairs in HEWL, calculated with help of the PATHWAYS model [24].

2. Experimental

2.1. Materials

Hen egg-white lysozyme (HEWL) of the highest purity available was purchased from Serva and was used as received. All other chemicals, NaN_3, Na_2HPO_4, $HClO_4$ and NaOH, were of the purest commercially available grade from Merck, and triacetylchitotriose (*N*-acetylglucosamine trimer; $(GlcNAc)_3$), was from Sigma. An *N'*-for-

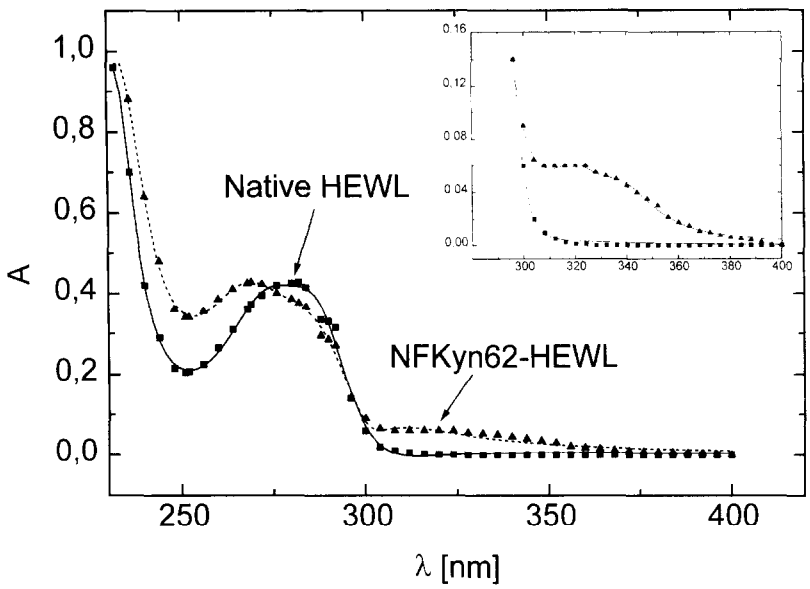

Fig. 1. Spectrophotometric control of oxidation of Trp62 indole side chain to *N'*-formylkynurenin in HEWL by ozone; the difference between the spectra of native HEWL and NFKyn62-HEWL corresponds to 1:1 conversion of 1 mol of Trp into NFKyn; in the inset is a part of the absorption spectrum due to the *O*-formylaminobenzoate group of NFKyn.

mylkynurenine derivative of HEWL, NFKyn62-HEWL, was obtained by selective and quantitative oxidation of Trp62 in HEWL with ozone [22,23]. The progress of the oxidation reaction was monitored spectrophotometrically (cf. Fig. 1) as the decrease in the protein's absorbance at 282 and 290 nm due to the indolyl chromophore, accompanied by an increase in absorption at 322 nm caused by formation of *O*-formylaminobenzoate group of kynurenine. The reaction was continued until the observed spectral changes indicated a 1:1 conversion of an indole moiety in HEWL into an *O*-formylaminobenzoate group of kynurenin. NFKyn62-HEWL thus obtained in aqueous solution was used in pulse radiolysis experiments without subsequent purification.

2.2. Methods

2.2.1. Pulse radiolysis

Pulse radiolysis experiments were performed at Risø National Laboratory with a 10-MeV HRC linear accelerator [25], equipped with a thermostated spectrophotometric cell, using 0.5-μs electron pulses and low doses of about 2 Gy per pulse. Absorbed doses were determined by ferrocyanide dosimetry. Intramolecular electron transfer in HEWL was induced by the highly selective oxidation of the indole side-chain of tryptophan residues to the indolyl-type $Trp^{\cdot}$ radicals with azide radicals, $N_3^{\cdot}$, formed within $< 1\,\mu s$ after the electron pulse by the reactions depicted in Eqs. (1)–(3) [5]:

$$H_2O \rightarrow e_{aq}^-, H^{\cdot}, {}^{\cdot}OH \quad (1)$$

$$e_{aq}^- + N_2O + H_2O \rightarrow N_2 + {}^{\cdot}OH + OH^- \quad (2)$$

$${}^{\cdot}OH + N_3^- \rightarrow N_3^{\cdot} + OH^- \quad (3)$$ [1]

The kinetics of the $Trp^{\cdot}$ decay and appearance of the $TyrO^{\cdot}$ radicals, as well as the initial (G_i) and

[1] In acidic solutions, the reaction scheme (Eqs. (1)–(3)) becomes complicated by the presence of HN_3 (pK 4.74) reacting with e_{aq}^- to form $HN_3^{\cdot-}$, which yields with proton donors also azide radicals in a process slower than the reaction depicted by Eq. (3) [26,27]. However, even at the lowest pH of 5.2 investigated here and 0.1 M azide concentration employed, the half-life of $N_3^{\cdot}$ formation in the latter reaction (ca. 1 μs), evaluated from the kinetic data of [26], is much shorter than that of ca. 5 μs found for oxidation of Trp residues in HEWL [4]. As a result the reaction depicted in Eqs. (4a) and (4b) is still rate-controlling under these conditions. Moreover, the effective yield of azide radicals could be expected to be similar to that in the neutral solution.

final (G_f) yields of their formation, were measured spectrophotometrically taking advantage of the large separation between the absorption spectra of the two species, with λ_{max} at 510 nm and 405 nm, respectively. The values of molar absorbance of these radicals in HEWL were assumed to be the same as those of the corresponding radicals in the free amino acids [28] (ϵ_{510}: 1800 and 70 M^{-1} cm^{-1} and ϵ_{405}: 300 and 2600 M^{-1} cm^{-1} for $Trp^{\cdot}$ and $TyrO^{\cdot}$, respectively). In acidic solutions, below pH 5.5, protonation of $Trp^{\cdot}$ (pK_a of about 5 [4]) yields $TrpH^{\cdot+}$ radicals (λ_{max} = 580 nm). Spectrophotometric quantification was performed also at 510 nm since the isosbestic point for the spectra of the two species is at this wavelength [29].

Pulse radiolysis experiments were carried out at a standard concentration of aqueous HEWL of 2 mg mL^{-1} ($\sim 1.4 \times 10^{-4}$ M); in some cases a higher concentration of 4 mg mL^{-1} ($\sim 2.8 \times 10^{-4}$ M) was employed. Under these conditions the electron-transfer reaction (Eq. (5)) was found independent of the protein concentration [3,4]. The solutions 0.1 M in N_3^- were bubbled with a high purity N_2O in order to convert hydrated electrons into hydroxyl radicals (see Eq. (2)). The pH of the solutions was adjusted either with phosphate buffer or by adding an appropriate amount of perchloric acid or sodium hydroxide.

In experiments with the HEWL–$(GlcNAc)_3$ 1:1 complex (K_{assoc} of the order of 1×10^5 M^{-1} in the whole pH range studied [30]), the concentration of $(GlcNAc)_3$ was 1.05×10^{-3} M and that of the enzyme $\sim 1 \times 10^{-4}$ M; thus more than 99 per cent of the HEWL molecules were complexed.

2.2.2. Selection of dominant LRET pathways

The relative importance of various molecular pathways of LRET between all possible $Trp^{\cdot}$/Tyr redox couples in HEWL was evaluated within the framework of the PATHWAYS model [24,31], implemented by J. Regan (Pathways 0.97), kindly provided by the authors of the program. The starting crystallographic coordinates for the protonated form of triclinic HEWL [32] were taken from the Brookhaven Protein Data Bank (entry 2LZT) [33].

According to the PATHWAYS model, a single electron-tunnelling pathway is defined as a combination of interacting bonds that link a donor (D) with an acceptor (A) via a combination of covalent (C), hydrogen-bonded (H) and/or van der Waals through-space (S) connections. The donor–acceptor electronic coupling for such a pathway, T_{DA}, is approximated as a product of the decay factors, ε, corresponding to all interacting bonds: $\Pi_i \varepsilon_i^C \Pi_i \varepsilon_i^H \Pi_i \varepsilon_i^S$. These unitless factors are appropriately parameterized. Each decay factor is associated with an effective distance: $d_{eff} = -\log \varepsilon$. Using graph theory the program searches for the shortest effective distance between donor and acceptor within a known protein network of bonded and non-bonded contacts. We applied essentially the original parametrization of the decay factors from the standard database. For aromatic ring bonds with delocalized wave functions (Trp, Tyr, Phe and His) a new parametrization, $\varepsilon^C = 0.95$, was introduced, to better account for their lower electron-transfer damping (J. Poznanski, unpublished work).

3. Results and Discussion

3.1. LRET in native HEWL at neutral pH

The initial yield of indolyl radicals, $G(Trp^{\cdot})_i$, in native HEWL at neutral pH proved to be one order of magnitude higher than that of phenoxyl radicals, $G(TyrO^{\cdot})_i$, (cf. Table 1). This is in general agreement with expectations based on the relative magnitude of the second-order rate constants for the reaction of $N_3^{\cdot}$ radicals with tryptophan and tyrosine as free amino acids [1], and as residues in short peptides [10]. Under the experimental conditions employed, the sum of these yields was close to the yield of azide radicals [6], $G(N_3^{\cdot}) \sim 6$, which indicates that other amino acid residues in HEWL were little affected, as has been observed earlier for a number of proteins [1,2]. The oxidation reaction was carried out under sufficiently low concentration of azide radicals and a large enough HEWL/$N_3^{\cdot}$ ratio (see Section 2.2.1) so that, according to the Poisson distribution, more than 99% of the lysozyme molecules oxidized by $N_3^{\cdot}$ attack could be expected to contain only a single oxidized site.

The synchronous decay of indolyl $Trp^{\cdot}$ and build-up of phenoxyl $TyrO^{\cdot}$ radicals in native HEWL (cf. Fig. 2, panels IA and IB) could be satisfactorily

Table 1
Analysis of temperature-independent radiation yields (G) of $Trp^{\cdot}$ and $TyrO^{\cdot}$ radicals in native HEWL, NFKyn62-HEWL and HEWL$(GlcNAc)_3$ complex

System	$G(Trp^{\cdot})_i$	$G(TyrO^{\cdot})_i$	$G(Trp^{\cdot})_f$	$G(TyrO^{\cdot})_f$	$\Delta G(Trp^{\cdot})_{i-f}$	$\Delta G(TyrO^{\cdot})_{i-f}$	LRET efficiency [a]
pH 7.3–7.4							
HEWL	5.6 (0.1)	0.6 (0.15)	0.6 (0.2)	3.2 (0.3)	4.9	2.6	0.5
NFKyn62-HEWL	2.3 (0.2)	1.2 (0.1)	1.1 (0.15)	1.7 (0.5)	1.2	0.5	0.4
HEWL$(GlcNAc)_3$ [b]	1.6 (0.2)	2.2 (0.3)	0.5 (0.1)	2.3 (0.3)	1.1	0.1	?
pH 5.2							
HEWL	3.7 (0.3)	0.7 (0.1)	0.7 (0.2)	4.5 (0.3)	3.0	3.8	?
NFKyn62-HEWL	2.0 (0.3)	0.8 (0.2)	1.0 (0.2)	2.1 (0.3)	1.0	1.3	?
HEWL$(GlcNAc)_3$	1.7 (0.1)	1.2 (0.3)	0.6 (0.15)	2.8 (0.3)	1.1	1.6	?

[a] LRET efficiency = $\Delta G(TyrO^{\cdot})_{f-i}/\Delta G(Trp^{\cdot})_{i-f}$. [b] Above 313 K $G(Trp)_i$ has increased to about 3.

represented as the first-order reaction (Table 2). Therefore LRET involved either one or more $Trp^{\cdot}$/Tyr redox couples, characterized by a similar rate constant. The oxidation (Eqs. (4a) and (4b)) and electron transfer (Eq. (5)) reactions can be thus summarized as follows:

$$N_3^{\cdot} + HEWL[6Trp, 3Tyr] \rightarrow N_3^- + HEWL[Trp^{\cdot}, 5Trp, 3Tyr] + H^+ \quad (4a)$$

$$N_3^{\cdot} + HEWL[6Trp, 3Tyr] \rightarrow N_3^- + HEWL[6Trp, TyrO^{\cdot}, 2Tyr] + H^+ \quad (4b)$$

$$HEWL[Trp^{\cdot}, 5Trp, 3Tyr] \rightarrow HEWL[6Trp, TyrO^{\cdot}, 2Tyr] \quad (5)$$

The relative probability with which particular Trp and Tyr residues in HEWL could be oxidized by $N_3^{\cdot}$, *RPOx*, was evaluated as $k_{4i}/\Sigma_i k_{4i}$, where k_{4i} is a second-order rate constant for the oxidation reaction (Eqs. (4a) and (4b)) for the respective free amino acid [1] multiplied by its relative exposure to the solvent, *RE* [21]. The calculated *RPOx* data (Table 3) strongly suggest that in the population of oxidized HEWL molecules those bearing a single $Trp62^{\cdot}$, $Trp63^{\cdot}$, or $Trp123^{\cdot}$ indolyl radical could constitute up to 90%, those bearing $Trp108^{\cdot}$ or $Trp111^{\cdot}$ about 8% and those with a single $TyrO^{\cdot}$ radical the remaining 2%. Inspection of the experimental $(G)_i$ values for the two radicals (Table 1) indicates that the actual yields of $Trp^{\cdot}$ and $TyrO^{\cdot}$ were somewhat lower and higher, respectively, than those expected on the basis of the calculated k_{4i} data. This might be due in part to the oversimplified assumptions underlying the calculation of the oxidation rates. For instance, no account was taken of the expected influence on k_{4i} of the dynamics of Trp and Tyr side-chains in HEWL, which differ considerably from each other in their root mean square (rms) fluctuations (cf. Table 3) [34]. Also the radical transformations for the pairs Trp111/Tyr23 and Trp108/Tyr23, Trp108/Tyr53 and Trp108/Tyr20 could contribute to the value of $G(TyrO^{\cdot})_i$ being higher than expected from the above considerations because they are up to four orders of magnitude faster than the Trp62/Tyr53 radical pair transformation. These four pairs are expected to form the most strongly electronically coupled pairs of redox couples in HEWL (see below). However, in view of the slight discrepancy between the experimental and calculated yields, we conclude that the experimental value of $G(Trp^{\cdot})_i$ consists, for the most part, of contributions from the indolyl radicals formed at the three selected Trp residues: Trp62 (~ 0.47) > Trp123 (~ 0.26 > Trp63 (~ 0.17).

The G_i values for both radicals (measured at the time when the $Trp^{\cdot}$ radicals reach the maximum yield after the 0.5 μs electron pulse) proved to be independent of temperature, which means that the oxidation of HEWL by $N_3^{\cdot}$ was completed by this time even at the lowest temperature investigated, viz. 283 K. The activation energy of LRET, E_a = 36.0 kJ mol^{-1}, derived from an Arrhenius plot of the k_5 kinetic data (Fig. 3) at pH 7.4, is 4–5 times higher than that found for activation of the same through-bond electron-transfer process in the longer peptides ($n = 4,5$) of the H-Tp-$(Pro)_n$-Tyr-OH series [13]. This strongly suggests that activation of LRET in HEWL involves thermal activation of some confor-

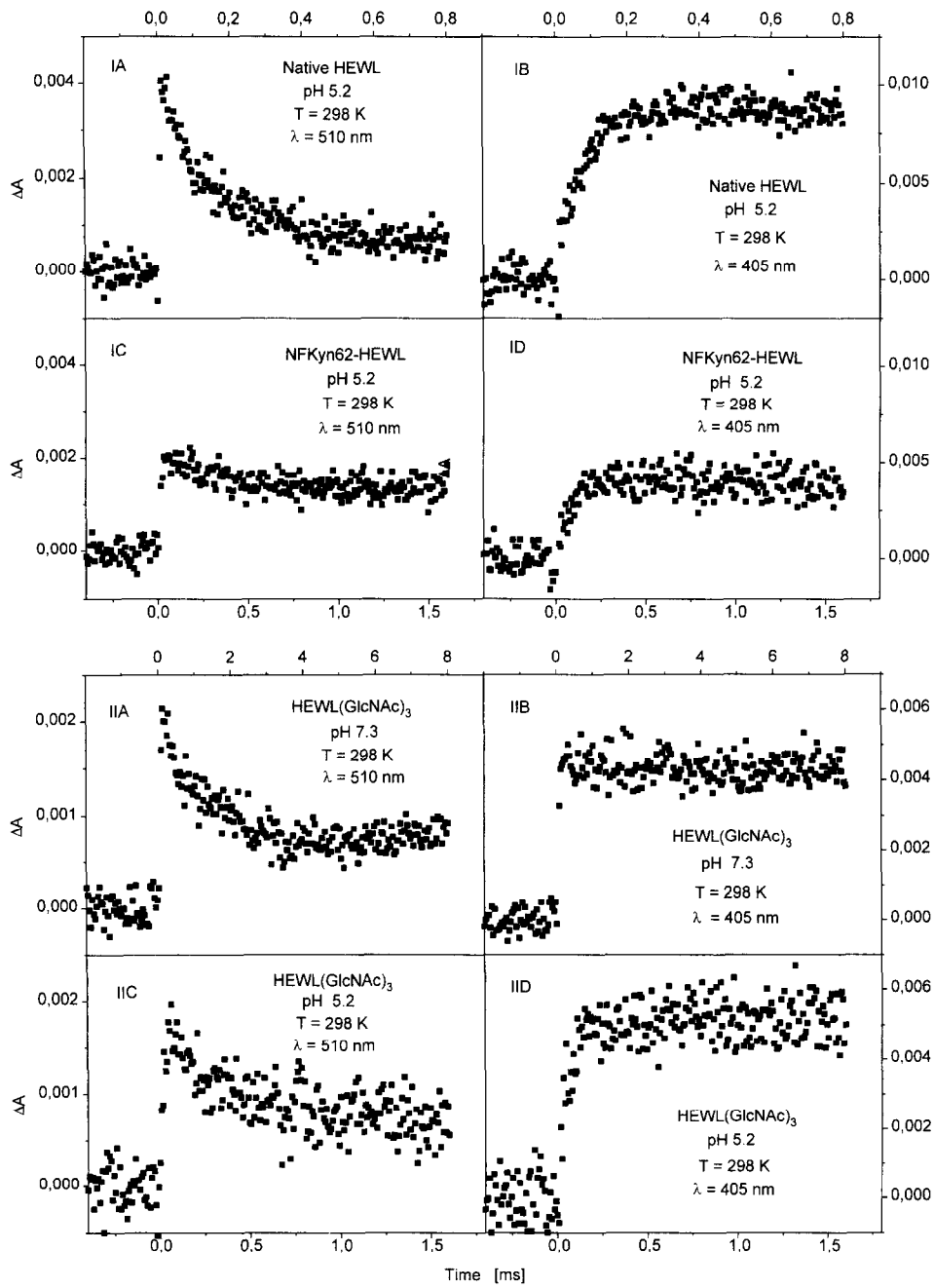

Fig. 2. Transient kinetics corresponding to decay of $Trp^{\cdot}$ (ΔA at 510 nm) and of $TyrO^{\cdot}$ (ΔA at 405 nm) radicals after pulse radiolysis triggering of the reaction depicted in Eq. (5) with $N_3^{\cdot}$ radicals at pH 5.2 in: native HEWL (panels IA and IB, 2.2 Gy per pulse), NFKyn62-HEWL (panels IC and ID, 2.4 Gy per pulse), and $HEWL(GlcNAc)_3$ (panels IIC and IID, 3 Gy per pulse), and at pH 7.3 in the latter complex (panels IIA and IIB, 2.5 Gy per pulse).

Table 2
Rate constants of intramolecular radical transformation $Trp^{\cdot} \rightarrow TyrO^{\cdot}$ in native HEWL, NFKyn62-HEWL and HEWL(GlcNAc)$_3$ complex

T(/K)	Native HEWL		Kyn62_HEWL		HEWL(GlcNAc)$_3$	
	k_5 (/s^{-1})					
	pH					
	5.2	7.3	5.2	7.3	5.2	7.3
283	7.6×10^3	2.9×10^2	1.0×10^3	6.3×10^2	2.5×10^3	4.1×10^2
288	7.9×10^3	3.9×10^2	1.5×10^3	6.9×10^2	2.9×10^3	4.4×10^2
293	8.3×10^3	5.0×10^2	2.6×10^3	7.3×10^2	4.4×10^3	4.8×10^2
298	8.7×10^3	6.3×10^2	3.9×10^3	8.0×10^2	5.2×10^3	5.1×10^2
303	9.4×10^3	7.2×10^2	5.3×10^3	8.6×10^2	7.6×10^3	5.6×10^2
308	1.2×10^4	9.9×10^2	6.5×10^3	9.2×10^2	8.3×10^3	7.4×10^2
313	1.6×10^4	1.2×10^3	9.8×10^3	1.0×10^3	1.1×10^4	1.1×10^3
318	2.5×10^4	1.4×10^3	1.5×10^4	1.1×10^3	1.5×10^4	1.3×10^3
323	3.5×10^4	1.8×10^3	2.0×10^4	1.1×10^3	1.8×10^4	1.4×10^3
328	4.1×10^4	–	3.0×10^4	–	2.0×10^4	1.8×10^3

mational fluctuations, specific to this protein. It is worth noting in this connection that in β-lactoglobulin the energy of activation of the reaction depicted in Eq. (5) is also very high, 45 kJ mol^{-1} [2].

3.2. Effect of pH on the rate of LRET in native HEWL

The rate of LRET in HEWL was found to increase with decreasing pH in the range 7–5 (Table 2, Fig. 4); as was observed earlier [2,4]. A closer inspection of the kinetic data indicates that k_5 increases very characteristically: the plot of k_5 against pH (Fig. 4) takes a sigmoidal shape down to about pH 5.2; below this pH value, there is a sharp increase in the rate of LRET. Only the latter part of the pH-dependence has been observed for the oligo-proline-bridged $Trp^{\cdot}$/Tyr redox couple ([12] and Bobrowski et al., in preparation; cf. inset in Fig. 4 showing the pH-dependence of k_{et} in H-Trp-(Pro)$_5$-Tyr-OH). This behaviour was attributed to protonation of $Trp^{\cdot}$ to $TrpH^{+\cdot}$ (pK_a may vary from ~4 to ~5 [4] depending on the location of Trp residue in a peptide chain). The latter radical gives rise to a faster LRET in the reaction with Tyr, due to a lower value of the free energy of reorganization, necessary for

Table 3
Relative probabilities of oxidation by $N_3^{\cdot}$ radicals (*RPOx*), relative accessibilities (*RE*) [21], and root-mean-square fluctuations [34] of Trp and Tyr residues in HEWL

Residue	Location	*RPOx*	*RE*	Fluctuations, rms (/nm)
Trp62	Cleft,top	0.470	0.54	0.2025
Trp123	Surface	0.260	0.29	0.0662
Trp63	Buried, behind Trp62	0.170	0.19	0.0737
Trp108	Cleft surface	0.043	0.05	0.0677
Trp111	Hydrophobic box	0.043	0.05	0.1175
Trp28	Hydrophobic box	0.000	0.00	0.0605
Tyr20	Surface	0.008	0.37	flip rate $> 10^{-2}$ s^{-1}
Tyr23	Surface	0.006	0.28	flip rate $> 10^{-2}$ s^{-1}
Tyr53	Buried	0.003	0.14	flip rate $> 10^{-2}$ s^{-1}

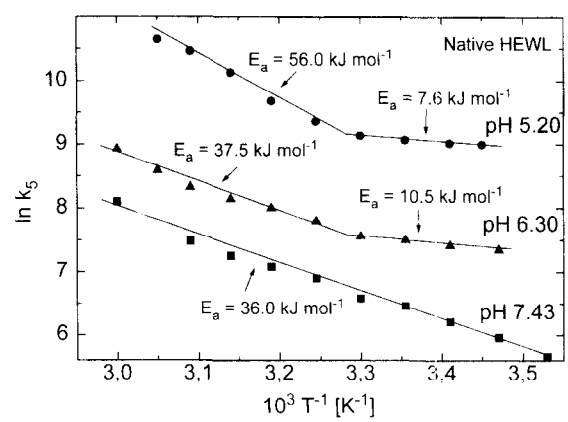

Fig. 3. Arrhenius plots for the temperature-dependence of the rate constant, k_5, of the reaction depicted by Eq. (5) for native HEWL at the pH values indicated; E_a are the corresponding energies of activation, derived from the slopes of the plots.

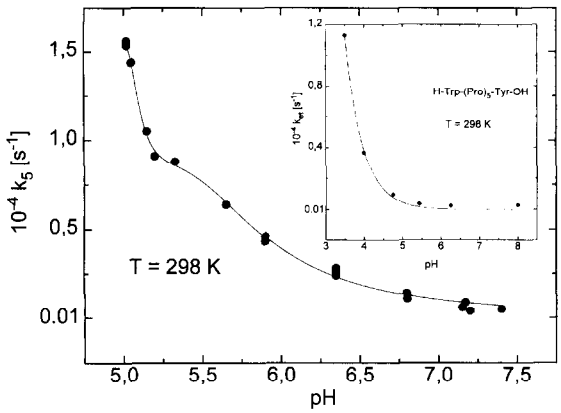

Fig. 4. Dependence of the rate constant for the reaction depicted in Eq. (5) on pH in native HEWL, and in H-Trp-(Pro)$_5$-Tyr-OH peptide (inset: dependence of k_{et} on pH, after K. Bobrowski et al., in preparation).

attainment of the transition state, as compared with the associated Trp[N]*/Tyr couple [35], in spite of the fact that Trp[NH]$^{\cdot+}$/Tyr has a lower electrochemical driving force for this process [2,4,12,35]. The sigmoidal part of the plot of k_5 against pH coincides with the pH region in which HEWL undergoes multiple protonation, first at the Glu35 site ($pK_a \sim 6.2$) and second, to a lesser extent, at the His15 ($pK_a \sim 5$), Asp101 ($pK_a \sim 4.7$) and Asp52 ($pK_a \sim 4.5$) sites [36]. Although upon protonation in this pH region there is no change in the Gibbs energy of HEWL unfolding [37], a number of local conformational adjustments in the protein structure does occur as a result of redistribution of partial electric charges in the immediate vicinity of the protonated residues [38]. An Arrhenius plot of $\ln k_5$ against T^{-1} at pH 5.2 (Fig. 3) is non-linear and indicates that the energy of LRET activation at about 300 K changes from a rather low value of 7.6 kJ mol^{-1} to a much higher one of 56 kJ mol^{-1}. The latter energy is higher than the value of 36.0 kJ mol^{-1} found for the activation of LRET in non-protonated HEWL at pH 7.4. The Arrhenius plot of the k_5 data collected at pH 6.3 has a similar shape to that at pH 5.2. This indicates that the apparent value of E_a varies with pH below pH 7.4. These observations are consistent with the occurrence of conformational changes in HEWL upon protonation and indicate involvement of a conformational control in LRET activation.

Also the initial yield of Trp$^{\cdot}$ formation, but not that of TyrO$^{\cdot}$, was found to be affected by HEWL protonation (cf. Table 1). The value of $G(\mathrm{Trp}^{\cdot})_i = 3.7$ determined at pH 5.2 is considerably lower than that of 5.6 measured at pH 7.4, in spite of expected similarity of $G(N_3^{\cdot})$ values at both pH values (cf. footnote 1). Contrary to this observation, in tryptophyl–tyrosyl dipeptides [6] the initial yield of phenoxy radicals was found to increase at low pH at the expense of the indolyl radical yield so that the total initial yield remained pH-independent. This might suggest that, upon protonation of HEWL, the accessibility of Trp62 and Trp63 residues to $N_3^{\cdot}$ radicals becomes smaller. The same observation has also been made for the $H^{\varepsilon 1}$ indolyl amide hydrogens of Trp63 and Trp108 in a hydrogen-exchange reaction and was ascribed to a higher conformational rigidity of the enzyme's substrate binding cleft as a consequence of the Glu35 and Asp52 ionization [38]. Since the reaction depicted in Eq. (5) is so rapid at pH 5.2, the efficiency of LRET probably approached its maximum value. The value of $G(\mathrm{TyrO}^{\cdot})_f$, 25% higher than that expected from the difference between the initial and final yields of Trp$^{\cdot}$, is probably more apparent than real because the yields were calculated under the assumption that the two radicals have similar molar absorbance values both in the form of free amino acids and when built into HEWL. Actually these values may be different and vary with location of the Trp and Tyr residues in the protein structure.

3.3. Effect of oxidation of Trp62 in HEWL to N′-formylkynurenine

Removal of Trp62 from HEWL by its selective and quantitative oxidation with ozone [22], described under Section 2, resulted in a large decrease in $G(\mathrm{Trp}^{\cdot})_i$ from 5.6 to 2.3 for the non-protonated form of NFKyn62-HEWL and from 3.7 to 2.0 for its protonated form (cf. Table 1). This was accompanied by a large increase in $G(\mathrm{TyrO}^{\cdot})_i$ in the non-protonated form. In the protonated form of NFKyn62-HEWL the initial yield of TyrO$^{\cdot}$ radicals was similar to that in native HEWL. In both forms, LRET of correspondingly lower yield and at a rate of similar order of magnitude but of different thermal activation energy was still observed (Figs. 2, 5 and 6,

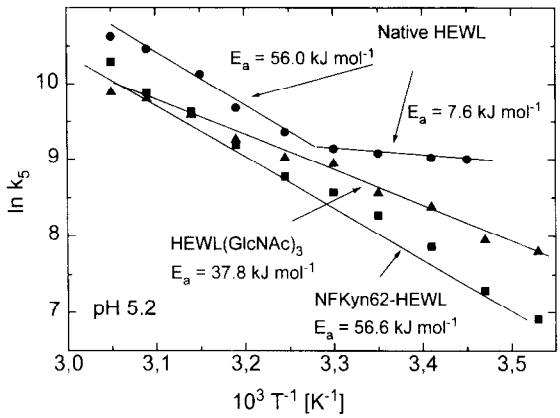

Fig. 5. Arrhenius plots for the temperature-dependence of the rate constant, k_5, of the reaction depicted in Eq. (5) at pH 5.2 for NFKyn62-HEWL and HEWL–(GlcNAc)$_3$ complex; E_a are corresponding energies of activation; the Arrhenius plot for the same reaction at pH 5.2 in native HEWL (from Fig. 3) is shown for comparison.

Table 2). All these observations firmly demonstrated that Trp62 is involved in, and contributes significantly to, LRET in native HEWL.

The lytic activity of NFKyn62-HEWL (with respect to *Micrococcus lysodeikticus* cells) has been found to be substantially lower than that of native HEWL [39], but CD and UV-difference spectroscopy investigations have revealed that the gross molecular

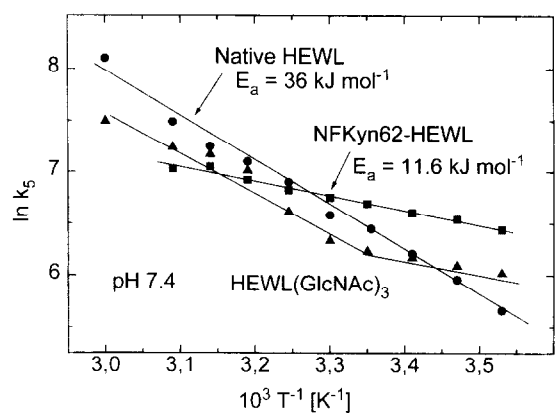

Fig. 6. Arrhenius plots for the temperature-dependence of the rate constant of the reaction depicted in Eq. (5) in NFKyn62-HEWL and for the rate of Trp$^{\cdot}$ decay in HEWL(GlcNAc)$_3$ complex at pH 7.4; E_a – corresponding energies of activation; the Arrhenius plot for k_5 in native HEWL at neutral pH (from Fig. 3) is shown for comparison.

conformation of the protein was only slightly affected by oxidation of Trp62 to *N'*-formylkynurenine. More detailed spectroscopic investigations on the Kyn62-HEWL derivative of NFKyn62-HEWL, obtained by hydrolytic removal of the *N'*-formyl group from the *N'*-formylkynurenine residue, fully confirmed that the gross structure of lysozyme was not significantly altered upon modification of the indole side chain of Trp62 to kynurenine. Nevertheless, this modification can be expected to introduce some local conformational changes in the immediate vicinity of this amino acid residue. Of the two tryptophan residues, Trp63 and Trp123, that can still be involved in LRET in NFKyn62-HEWL, only the conformational freedom of the neighbouring Trp63 could be significantly affected by the oxidation of Trp62. This should manifest itself in the Arrhenius plot of k_5 for NFKyn62-HEWL. Indeed, the slope of this plot for the non-protonated form of the modified protein (Fig. 6) corresponds to a threefold lower value of the activation energy of LRET as compared with that found for native HEWL. This strongly suggests that it is Trp63 that is now mainly involved in the observed electron transfer. The rate of LRET in NFKyn62-HEWL at pH 5.2 is lower than in native HEWL in the whole range of temperatures investigated (Table 2), but the energy of LRET activation does not vary with temperature, E_a = 56.6 kJ mol^{-1}, and closely resembles that of HEWL above 300 K (Fig. 5). One may thus conclude that the low energy of LRET activation, E_a = 7.6 kJ mol^{-1}, found for protonated HEWL below 300 K, but not in its NFKyn62 derivative, can be ascribed to a redox couple involving Trp62$^{\cdot}$. Such a low value of E_a would be fully consistent with the highly fluid conformational dynamics of the Trp62 indolyl side chain (cf. Table 3).

3.4. Effect of binding to HEWL of the (GlcNAc)$_3$ inhibitor

Binding of the (GlcNAc)$_3$ inhibitor to the substrate cleft of HEWL in either form, neutral or protonated, caused a further drop in the initial value of G(Trp$^{\cdot}$)$_i$ relative to the respective forms of NFKyn62-HEWL (Table 1).

The inhibitor binds specifically to the A, B and C sites of the active site cleft in a manner similar to the

type of productive binding of *N*-acetyloglucosamine hexamer [40,41]. There are clear indications that the conformation of HEWL, both in the crystal state [42] and in aqueous solution [43], is affected by binding of $(GlcNAc)_3$. In the complex, the terminal residue of the inhibitor forms hydrogen-bonds between the NH and carbonyl oxygens of the *N*-acetyl side-groups and the main chain CO and NH groups of Ala107 and Ileu59, respectively, and between O(6) and O(3) atoms and the NH groups of the indole side chains of Trp62 and Trp63, respectively. The inhibitor connects the two sides of the binding cleft in a cooperative way [21], so that both Trp62 and Trp63 (as well as Trp108) which are located in the substrate/inhibitor binding cleft, are completely shielded from the solvent by the bound inhibitor molecule, and thus are inaccessible to $N_3^{\cdot}$ radicals.

Moreover, the rate of exchange of the bound inhibitor is of the order of $3 \times 10^2\ s^{-1}$ [43] which is slow on the time-scale of the reaction (Eq. (5)). Thus, the measured values of $G(Trp^{\cdot})_i$ for the inhibitor complex should be attributed, for the most part, to oxidation of Trp123, the only Trp residue in the complex with significant solvent accessibility ($RE = 0.29$). Since in free HEWL only three Trp residues, 62, 63 and 123, contribute substantially to $G(Trp^{\cdot})_i$, the observed decrease in this yield upon binding of the inhibitor to the neutral form of HEWL should quantitatively reflect the inaccessibility of Trp62 and Trp63 to $N_3^{\cdot}$ attack. On the other hand, the initial yield of $TyrO^{\cdot}$ in the complex was several times higher than $G(TyrO^{\cdot})_i$ in free HEWL and its NFKyn62 derivative. As a result, the total initial yield of the two radicals, $G(Trp^{\cdot})_i + G(TyrO^{\cdot})_i$, was close to 60% of the values determined for free HEWL, and was comparable with those found for NFKyn62-HEWL (cf. Table 1). Such an increase in $G(TyrO^{\cdot})_i$ upon removal of the easily oxidizable Trp sites is understandable. In these circumstances, the two solvent-accessible surface Tyr residues in the $HEWL(GlcNAc)_3$ complex, viz. Tyr20 and Tyr 23, compete effectively for $N_3^{\cdot}$ with a limited number of potentially oxidizable Trp residues.

In the protonated $HEWL(GlcNAc)_3$ complex, the reaction depicted by Eq. (5) was still observed (Fig. 2). However, the first-order rate constant, k_5, was somewhat lower than for the free enzyme over the whole range of temperatures studied (Table 2). This could be expected for the $Trp123^{\cdot}/Tyr23$ redox couple on the basis of theoretical evaluation of the electronic couplings between all possible $Trp^{\cdot}/Tyr$ pairs in HEWL (see below). Also the energy of LRET activation, $E_a = 37.8\ kJ\ mol^{-1}$, derived from the linear Arrhenius plot of k_5 data (Fig. 5), proved intermediate between the two E_a values obtained from the non-linear plot for LRET activation in free protonated HEWL.

Binding of the inhibitor is known to perturb the pK_a values of a number of amino acid residues, and in particular it shifts that of Glu35 to about 6.5 [44]. It also decreases the exchange rates of all protons and thus also the conformational dynamics of the various domains of the protein [21]. The observed effects of $(GlcNAc)_3$ binding on the rate of reaction (Eq. (5)) and its activation energy can thus be rationalized in terms of the conformational changes induced in HEWL by binding of the inhibitor.

The pulse radiolysis data obtained for the $HEWL(GlcNAc)_3$ complex at pH 7.3 (Fig. 2, Tables 1 and 2) did not provide firm evidence for the occurrence of $Trp^{\cdot} \rightarrow TyrO^{\cdot}$ conversion. Although the decay of $Trp^{\cdot}$ radicals with a first-order rate constant similar to that in free HEWL was clearly observed (Fig. 2, Table 2), it was not accompanied by a simultaneous build-up of phenoxy radicals. The high initial yield of $TyrO^{\cdot}$ remained unchanged until the completion of $Trp^{\cdot}$ depletion at the end of the observation time window of 80 μs, so that it was practically equal to $G(TyrO^{\cdot})_f$. The value of the latter was similar to those found in the other systems studied (Fig. 2, Table 1). If LRET were to occur in this system, the apparently constant level of $TyrO^{\cdot}$ radicals might have resulted from compensation of two opposing processes of similar rate — their formation, due to the intramolecular oxidation of Tyr by $Trp^{\cdot}$, and decay by an unknown reaction. At present, we are not able, however, to propose any mechanism responsible for such a fast decay of $TyrO^{\cdot}$.

3.5. Theoretical evaluation of the dominant LRET pathways between potential $Trp^{\cdot}/Tyr$ redox pairs in native HEWL

To evaluate which of the potential $Trp^{\cdot}/Tyr$ redox pairs in HEWL can be expected to contribute significantly to the LRET observed, we applied the

PATHWAYS model [24,31] which identifies the dominant electron-tunnelling pathways in proteins, i.e. a combination of covalent, hydrogen-bonding and through-space non-bonding interactions responsible for the donor–acceptor coupling. According to this model, differences in electron-transfer rates for a given redox pair are expected to be due to differences in their electronic coupling via the dominant physical pathways of the system. This model has already been used successfully to predict the relative rates of electron transfer in a number of ruthenium-derivatized redox proteins of known three-dimensional structure [24,45].

The calculated couplings corresponding to these pathways, collected in Table 4, indicate that the most strongly coupled Trp/Tyr pairs are those which include Trp residues buried deeply in the protein matrix and thus practically inaccessible to azide radical attack: Trp111 and Trp28 (located in the hydrophobic box, *RE*: 0.05 and 0.00, respectively), and Trp108 (substrate cleft, $RE = 0.05$). The next strongly coupled group of the redox pairs includes the most solvent-accessible Trp62 ($RE = 0.54$) and Trp63 ($RE = 0.19$), located on the surface of the substrate-binding cleft, and Trp123 ($RE = 0.29$) on the opposite side of the protein surface. We have demonstrated in this study that the radical state of Trp62 contributes significantly to the observed LRET, and participation of the other two tryptophans in this process has been indirectly implicated. Trp62 and Trp63 are strongly coupled only to Tyr53 along the pathways depicted in Fig. 7. The rate constants of LRET along these pathways, proportional to the square of the electronic coupling, should not differ by more than a factor of about 2. Trp63 is also coupled to Tyr20 and Tyr23, but with a much lower strength so that corresponding rates of LRET should be more than two orders of magnitude lower than that of the Trp63/Tyr53 pair. The Trp123/Tyr23 pair is characterized by an electronic coupling of intermediate strength between the former two (cf. Table 4) along a pathway which includes 3 through-space electron jumps (cf. Fig. 7). The rate of LRET between the members of this pair can thus be expected to be slower by a factor of 24 and 57 relative to Trp62/Tyr53 and Trp63/Tyr53 couples, respectively.

The results of the theoretical evaluation of the electronic coupling between various Trp/Tyr potential redox pairs in HEWL provided information concerning which of these pairs and dominant pathways can be involved in LRET. They also support some of

Table 4
Dominant electron-transfer pathways between potential Tyr/Trp donor–acceptor pairs in hen egg-white lysozyme, calculated according to the PATHWAYS model [24,31]

Donor	Acceptor	Pathway [a]	Distance [b] (/nm)	T_{DA}
Tyr23	Trp62	-(S)-Val99-(C)-Ile98-(S)-Trp63-(C)-	3.59	4.83×10^{-7}
Tyr53	Trp123	-(C)-Gly54-(C)-Ile55-(S)-Ser36-(H)-Ala32-(C)-Lys33-(S)-	3.55	1.39×10^{-6}
Tyr20	Trp62	-(S)-Lys96-(C)-Lys97-(S)-Trp63-(C)-	3.15	1.59×10^{-6}
Tyr53	Trp111	-(H)-Gln57-(C)-Leu56-(H)-Trp108-(S)-	3.14	5.72×10^{-6}
Tyr20	Trp123	-(S)-Trp28-(C)-Val29-(S)-	2.95	5.91×10^{-6}
Tyr53	Trp28	-(H)-Gln57-(C)-Leu56-(H)-Trp108-(S)-	3.29	1.85×10^{-5}
Tyr23	Trp63	-(S)-Val99-(C)-Ile98-(S)-	2.36	3.19×10^{-5}
Tyr23	**Trp123**	-(S)-Trp111-(S)-Cys115-(S)-Cys30-(H)-	**2.10**	$\mathbf{7.52 \times 10^{-5}}$
Tyr20	Trp63	-(S)-Lys96-C-Lys97-(S)-	2.14	9.45×10^{-5}
Tyr20	Trp111	-(S)-Tyr23-(S)-	2.49	2.36×10^{-4}
Tyr53	**Trp62**	-(S)-Ser60-(C)-Arg61-(C)-	**2.10**	$\mathbf{3.69 \times 10^{-4}}$
Tyr53	**Trp63**	-(S)-Ser60-(C)-Asn59-(S)-	**1.70**	$\mathbf{5.68 \times 10^{-4}}$
Tyr20	Trp108	-(S)-Val99-(S)-	1.90	7.55×10^{-4}
Tyr53	Trp108	-(H)-Gln57-(C)-Leu56-(H)-	1.86	9.79×10^{-4}
Tyr23	Trp108	-(H)-Met105-(S)-	1.31	5.20×10^{-3}
Tyr20	Trp28	-(S)-	1.21	1.08×10^{-2}
Tyr23	Trp28	-(S)-	0.99	2.67×10^{-2}
Tyr23	Trp111	-(S)-	1.03	3.90×10^{-2}

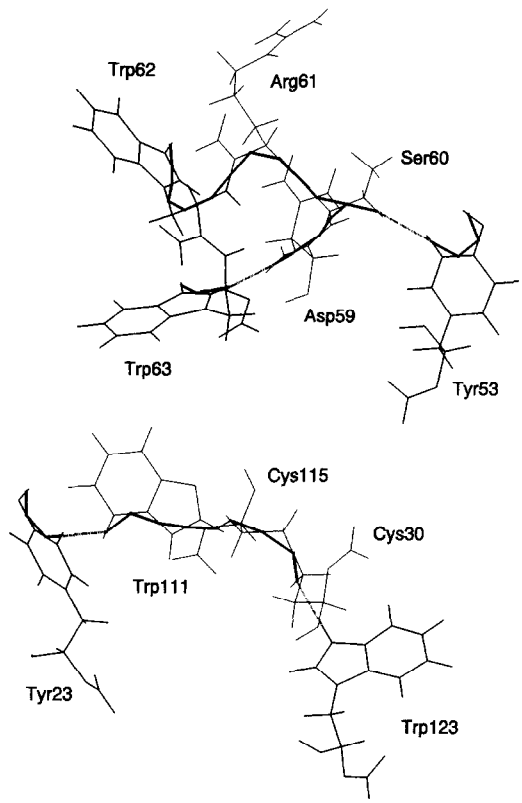

Fig. 7. The dominant LRET pathways between Trp62/Tyr53, Trp63/Tyr53 and Trp123/Tyr23 potential donor–acceptor couples in native HEWL, selected with the help of the PATHWAYS model and software [24,31]; light full lines – skeletons of amino acid residues indicated, bold full lines – tunnelling of electron through peptide backbone covalent bonds, dashed lines – through-space electron jumps between atoms in van-der-Waals contact.

the conclusions derived from experimental data on involvement of Trp62 and Trp63 in LRET and the similarity of the rate constants for LRET between the Trp62/Tyr53 and Trp63/Tyr53 couples, and to some extent also between the former two and the Trp123/Tyr23 couple. These conclusions were drawn on the basis of a comparison of the initial yields of $Trp^{\cdot}$ radicals and the kinetics of LRET in HEWL and NFKyn62-HEWL. The values of the electronic coupling calculated for the dominant pathways between the redox centres in question were obtained for the static crystal structure of HEWL. Since the present version of the PATHWAYS model does not take into account the dynamics of protein structure, electronic couplings for pathways involving a number of through-space jumps could be severely underestimated. This point of view is fully supported by the results of our molecular dynamics studies on variation in time of distances between atoms involved in through-space electron jumps and, calculated therefrom, time-dependence of the square of the electronic coupling, T^2_{DA}, for selected LRET pathways in question (Poznanski; manuscript in preparation). In general, they showed that variation of T^2_{DA}, governed for the most part by the presence of through-space electron jumps along a pathway, increases by approximately one order of magnitude per jump. Evolution in time of the normalized value of T^2_{DA} for the Tyr23...Trp123 pathway (Fig. 8) indicates that a very low time-averaged value of this parameter, corresponding to 0.03 of the maximum T^2_{DA} value (median: 0.0044) may occasionally attain a much higher momentary value. The results obtained indicate that electron transfer is strongly coupled to thermal motions of the protein matrix, so that any interpretation of LRET kinetics based on the static protein structure can be considered, at best, as semi-quantitative.

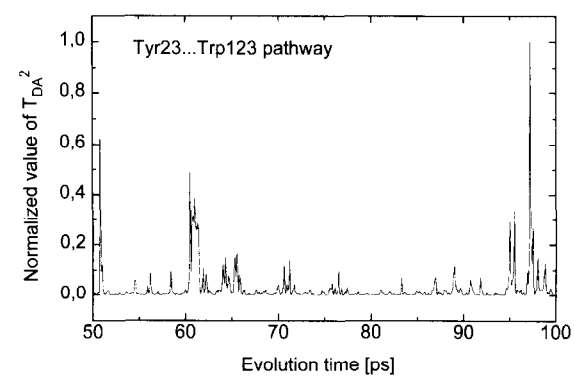

Fig. 8. Variation in time of the square of the electronic coupling, T^2_{DA}, normalized to its maximum momentary value, for the Tyr23...Trp123 dominant LRET pathway in HEWL; time averaged value of the parameter equals 0.03 of its maximum value, and median value is 0.0044. Momentary values of the T^2_{DA} parameter were calculated according to the PATHWAY model under the assumption of time-invariant pathway topology, and time-dependent interatomic distances for through-space electron jumps were obtained from the last 50 ps of molecular dynamics simulations for HEWL in vacuum, after thermal equilibration of the system at 300 K. In simulations, the TRIPOS force field with Kollman's all-atom charges, 1 fs step and 100 fs sampling time were used (from J. Poznanski, in preparation).

3.6. Conformational control of LRET in HEWL

The much larger energy of activation for the reaction depicted in Eq. (5) in HEWL at neutral pH compared with that for the analogous reaction across the oligoproline bridge in Trp-$(Pro)_n$-Tyr peptides [12], as well as the apparent variation of E_a with temperature in the protonated form of HEWL, led us to postulate conformational control of LRET by the protein matrix. In general, it can be expected that thermally induced local fluctuations in a protein matrix may help to increase the electronic coupling between a donor–acceptor pair by allowing the intervening peptide backbone and the pair itself to attain a more favourable conformation for larger overlap of the bridging atomic and molecular electron orbitals. These fluctuations should have a particularly strong influence on through-space couplings between non-bonded and hydrogen-bonded atoms, as shown in Section 3.5 by dynamic simulation of variation in time of the square of electronic coupling along pathways including a different number of non-bonded connections. Temperature studies on the kinetics of hydrogen exchange in HEWL [38,46,47] have identified the occurrence of two distinct mechanisms for exchange, one (i) characterized by a high activation energy of the order of 400 kJ mol^{-1} directly associated with the cooperative thermal unfolding of the protein, and the second (ii) of lower activation energy associated with local fluctuations in the protein structure. The activation energies for indole NH hydrogen exchange, consistent with the second mechanism, are about 55 kJ mol^{-1} for Trp63 and much below this value for Trp62 [46]. They are thus very close to those determined for LRET in HEWL. It seems thus very probable that conformational fluctuations (ii) involved in activation of hydrogen exchange in HEWL contribute also to activation of LRET between $Trp^{\cdot}$/Tyr redox pairs in this protein. The very low value of $E_a = 7.6$ kJ mol^{-1}, ascribed to fluctuation of Trp62 in the protonated form of HEWL, is very close to that found in longer peptides of the H-Trp-$(Pro)_n$-Tyr-OH group [13]: 8 and 7 kJ mol^{-1} for $n = 4$ and $n = 5$ peptides, respectively. Such a low energy of activation is thus characteristic of practically free motion of a Trp indolyl side chain [34]. The observed variation of the activation energy of LRET in HEWL with temperature at pH values below 7.4 seems to be connected with the presence of multiple forms of protonated HEWL molecules, the contribution of particular species in the total population of HEWL molecules being pH-dependent.

References

[1] E.J. Land and W.A. Prütz, Int. J. Radiat. Biol., 36 (1979) 75.
[2] J. Butler, E.J. Land, W.A. Prütz and A.J. Swallow, Biochim. Biophys. Acta, 705 (1982) 150.
[3] K. Bobrowski, J. Holcman and K.L. Wierzchowski, Free Radical Res. Commun., 6 (1989) 235.
[4] M. Weinstein, Z.B. Alfassi, M.R. DeFelippis, M.H. Klapper and M. Faraggi, Biochim. Biophys. Acta, 1076 (1991) 173.
[5] W.A. Prütz and E.J. Land, Int. J. Radiat. Biol., 36 (1979) 513.
[6] W.A. Prütz, E.J. Land and R.W. Sloper, J. Chem. Soc. Faraday Trans. 1, 77 (1981) 281.
[7] J. Butler, E.J. Land, W.A. Prütz and A.J. Swallow, J. Chem. Soc. Chem. Commun., (1986) 348.
[8] W.A. Prütz, F. Siebert, J. Butler, E.J. Land, A. Menez and T. Montenay-Garestier, Biochim. Biophys. Acta, 705 (1982) 139.
[9] K. Bobrowski, K.L. Wierzchowski, J. Holcman and M. Ciurak, Studia Biophysica, 122 (1987) 23.
[10] M. Faraggi, M.R. DeFelippis and M.H. Klapper, J. Am. Chem. Soc., 111 (1989) 5141.
[11] M. Faraggi and M.H. Klapper, in C. Ferradini and J.-P. Jay-Cerin (Eds.), Excess Electrons in Dielectric Media, CRC Press, Boca Raton, 1990, p. 397.
[12] K. Bobrowski, K.L. Wierzchowski, J. Holcman and M. Ciurak, Int. J. Radiat. Biol., 57 (1990) 919.
[13] K. Bobrowski, J. Holcman, J. Poznanski, M. Ciurak and K.L. Wierzchowski, J. Phys. Chem., 96 (1992) 10036.
[14] K. Bobrowski, J. Poznanski, J. Holcman and K.L. Wierzchowski, in J.F. Wishart and D.G. Nocera (Eds.), Photochemistry and Radiation Chemistry, ACS Adv. Chem. Ser., 1996, in press.
[15] R.C. Prince and G.N. George, TIBS 15 (1990) 170.
[16] M. Sivaraja, D.B. Goodin, M. Smith and B.M. Hoffman, Science, 245 (1989) 738.
[17] J.E. Erman, L.B. Vitello, J.M. Mauro and J. Kraut, Biochemistry, 28 (1989) 7992.
[18] R.J. Debus, B.A. Barry, I. Sithole, G.T. Babcock and L. McIntosh, Biochemistry, 27 (1988) 9071.
[19] P. Reichard, Biochemistry, 26 (1987) 3245.
[20] R. Karthein, R. Dietz, W. Nastainczyk and H.H. Ruf, Eur. J. Biochem., 171 (1988) 313.
[21] C.C.F. Blake, D.E.P. Grace, L.N. Johnson, S.J. Perkins and D.C. Phillips, Molecular Interactions and Activity in Proteins, Ciba Foundation, London, 1978, p. 135.
[22] J. Kuroda, F. Sakiyama and K. Narita, J. Biochem., 78 (1975) 641.

[23] F. Sakiyama and R. Natsuki, J. Biochem., 79 (1976) 225.
[24] D.N. Beratan, J.N. Betts and J.N. Onuchic, Science, 252 (1991) 1285.
[25] K. Sehested, J. Holcman and E.J. Hart, J. Phys. Chem., 87 (1983) 1951.
[26] Z.B. Alfassi, W.A. Prütz and R.H. Schuler, J. Phys. Chem., 90 (1986) 1198.
[27] D.J. Deeble, B.J. Parsons and G.R. Alastair Johnson, Radiat. Phys. Chem. 36 (1990) 487.
[28] R.V. Bensasson, E.J. Land and T.G. Truscott, Flash Photolysis and Pulse Radiolysis, Pergamon Press, Oxford, 1983.
[29] M.L. Posener, G.E. Adams and P. Wardman, J. Chem. Soc. Faraday Trans. 1, 72 (1976) 2231.
[30] . K. Teshima, S. Kuramitsu, K. Hamaguchi, F. Sakiyama, K. Mizuno and N. Yamasaki, J. Biochem., 87 (1980) 1015.
[31] J.N. Betts, D.N. Beratan and J.N. Onuchic, J. Am. Chem. Soc., 114 (1992) 4043.
[32] M. Ramanadham, L.C. Sieker and L.H. Jensen, Acta Crystallogr. Sect. A: 43 (Suppl.) (1987) 13.
[33] F.C. Bernstein, T.F. Koetzle, G.B. Williams, G.F. Meyer, M.D. Price, J.R. Rodgers, O. Kennard, T. Shimanouchi and M. Tasumi, J. Mol. Biol., 122 (1977) 535.
[34] T. Ichiye and M. Karplus, Biochemistry, 22 (1983) 2884.
[35] M.R. DeFelippis, C.P. Murthy, F. Broitman, D. Weinraub, M. Faraggi and M.H. Klapper, J. Phys. Chem., 95 (1991) 3416.
[36] M. Delepierre, C.M. Dobson, M.A. Howarth and F.M. Poulsen, Eur. J. Biochem., 145 (1984) 389.
[37] W. Pfeil and P.L. Privalov, Biophys. Chem., 4 (1976) 41.
[38] M. Delepierre, C.M. Dobson, M. Karplus, F.M. Poulsen, D.J. States and R.E. Wedin, J. Mol. Biol., 197 (1987) 111.
[39] N. Yamasaki, T. Tsujita, T. Eto, S. Masuda, K. Mizuno and F. Sakiyama, J. Biochem., 86 (1979) 1291.
[40] T. Imoto, L.N. Johnson, A.C.T. North, D.C. Phillips and J.A. Rupley, in P.D. Boyer (Ed.), The Enzymes, Academic Press, New York, 1972, p. 665.
[41] S.K. Banerjee, E. Holler, G.P. Hess and J.A. Rupley, J. Biol. Chem., 250 (1975) 4355.
[42] C.C.F. Blake, L.N. Johnson, G.A. Mair, A.C.T. North, D.C. Phillips and V.R. Sarma, Proc. Roy. Soc. London Ser. B: 167 (1967) 378.
[43] K.J. Lumb, J.C. Cheetham and C.M. Dobson, J. Mol. Biol., 235 (1994) 1072.
[44] Y. Nakae, E. Ryo, S. Kuramitsu, K. Ikeda and K. Hamaguchi, J. Biochem., 78 (1975) 589.
[45] D.N. Beratan, J.N. Onuchic, J.N. Betts, B.E. Bowler and H.B. Gray, J. Am. Chem. Soc., 112 (1990) 7915.
[46] R.E. Wedin, M. Delepierre, C.M. Dobson and F.M. Poulsen, Biochemistry, 21 (1982) 1098.
[47] T.G. Pedersen, N.K. Thomsen, K.V. Andersen, J.C. Madsen and F.M. Poulsen, J. Mol. Biol., 230 (1993) 65.